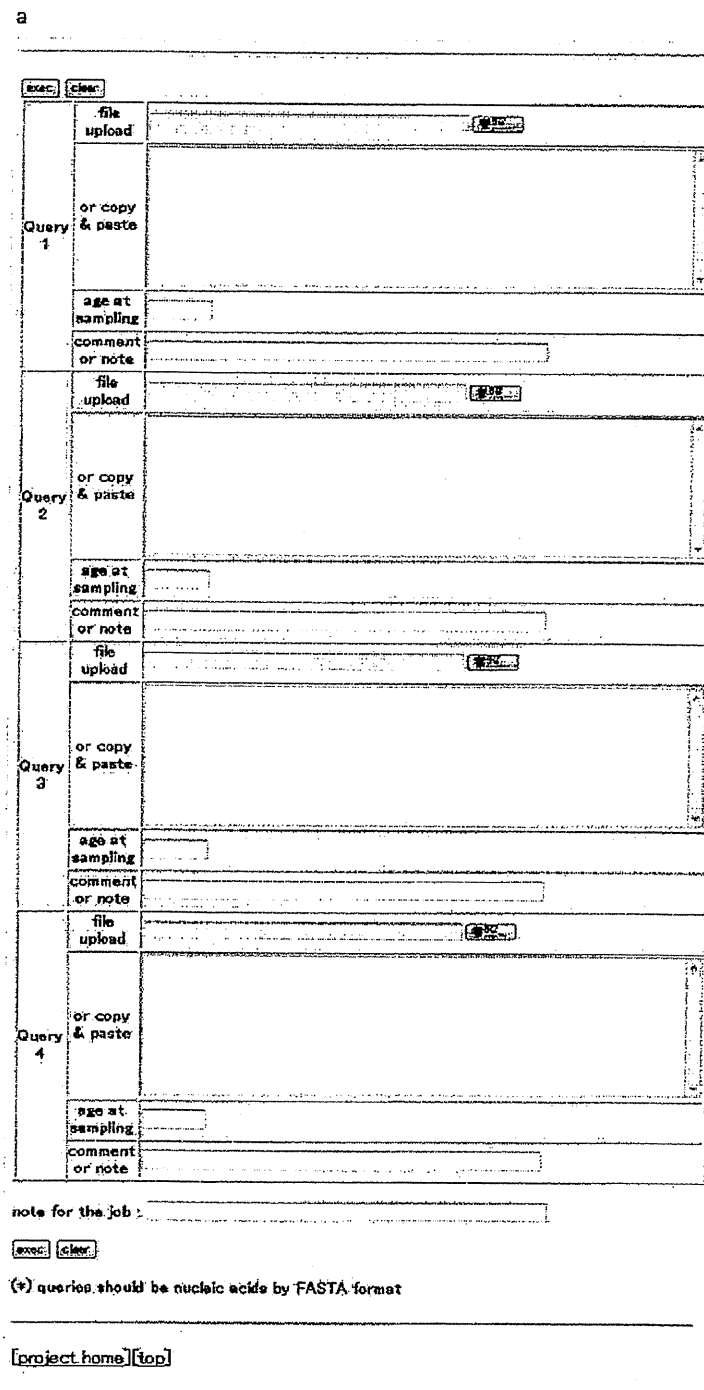

Figure 1 WWW-based user interface. To avoid bias such as age and selective pressure of antiviral treatment, adjustment parameters are prepared to obtain appropriate results. (a) The input field of query sequences and patient's age when serum was collected is shown. (b) The upper field configures masked sites for the elimination of drug-resistant sites. The lower field is a mutation rate of hepatitis B virus (HBV).

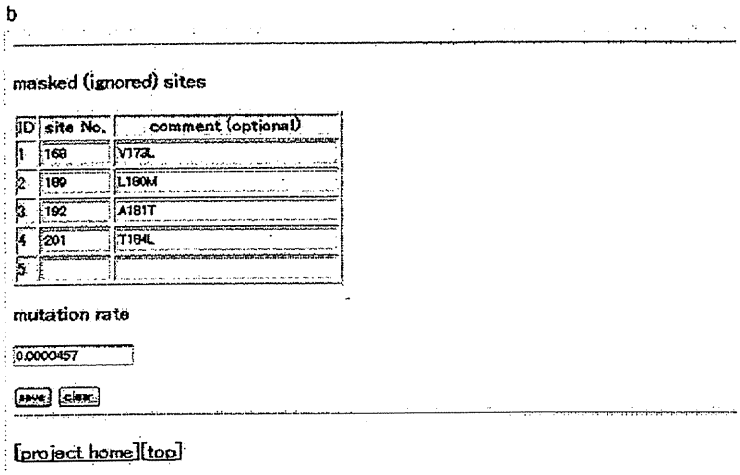

Figure 1 *Continued.*

RESULTS

Preparation of reference data

A DATASET OF all HBV S gene sequences that contain sequence variations in Japanese patients was retrieved from the HVDB[21] for reference sequences to classify suspicious samples of intrafamilial transmission. A representative sequence was selected among the same sequences in a cluster to optimize phylogenetic analysis. Full annotations of all sequences were also extracted from HVDB. The data of major genotypes were registered into the system. The results of the dataset were shown in Table 2.

Calculation for the classification of new sequences

New sequences input in query columns were calculated and then classified by the following process (Fig. 1a). The query sequences were added to the reference database described above, and the overall sequences were multiple-aligned by CLUSTAL W[22]. More precise alignment than direct alignment among queries was obtained regardless of the sequence quality of queries. Then, the genetic distance matrix was calculated from the alignment with the six-parameter method,[23] using only the sites shared by all the sequences. Finally the phylogenetic tree was constructed from the matrix using the neighbor-joining method,[24] which showed the relation among the queries, between query and published entries. The above calculation was conducted without using nucleotide positions of drug-induced resistant mutations to avoid selective pressure of antiviral treatment (Fig. 1b). As shown in Figure 1b, the mutation site of Lamivudin, Adefovir diproxil, and Entecavir resistance were masked in the present study along with the previous study.[25,26] We have estimated the substitution rate for HBV to be 4.57×10^{-5} per site per year.[27] In addition, the adjustment of age factor was calculated in consideration of genetic distance between queries for precise phylogenetic analysis (Fig. 1a). The distribution of nucleotide differences could be generally approximated by Poisson distribution and its average difference site number in the PCR amplicon of this study was 4.67 bases. The probability that two independent samples had the same sequence by chance was estimated to be less than 1%, and then the false positive data were seldom output in the intrafamilial transmission case. This system showed a sensitivity of 100% by calculating independent data retrieved from Osiowy *et al.*[28] The paper provided sequence data of a 25-year period obtained from eight asymptomatic carriers of the HBV genotype B in 1979 and 2004. For the calculation of the specificity, random sampling was performed using HVDB data. The specificity of this system was 98.6% by sampling 72 data.

Users interface

We also developed a WWW-based user interface to conduct the analysis easily. Researchers get two types of results in one analysis after they upload two or more query sequences through WWW browsers. One is a report of nucleotide difference number between

queries. This shows an indication of whether queries are similar enough or not. The other is a phylogenetic tree that shows the relation among queries and reference data.

Determination of transmission route in family cases

Four independent samples of chronic hepatitis B obtained from our hospital were tested before the analysis of suspicious intrafamilial transmission cases. Each of these four sequences was classified into distinct cluster (data not shown). As the E-PAS worked well, the analysis of suspicious intrafamilial transmission cases was examined to reveal whether two (or more) sequences obtained from a family were from intrafamilial transmission or not. The analysis was carried out by the process described above. The queries in the multiple alignments were compared between queries to count different nucleotide sites. Then, the comparison is done using the high-quality regions of the queries by ignoring ambiguous base ("N" base) sites. If three or more queries of a family were entered in the system, the comparison was calculated for each pair of queries. Table 1 shows characteristics of patients

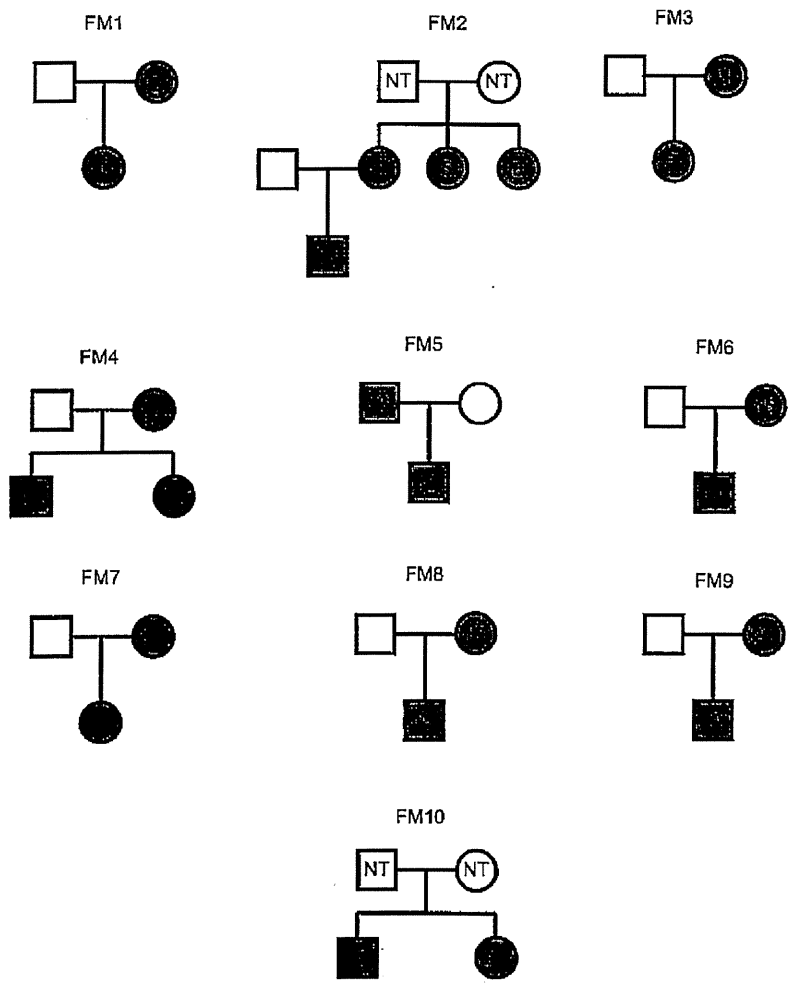

Figure 2 Family trees for 10 families with clustering hepatitis B virus (HBV) infection. Gray color indicates HBsAg positive, and white color indicates hepatitis B surface antigen (HBsAg) negative. Patients without HB antigen information are described as not tested (NT). Squares indicates male sex, circles indicates female sex.

Japanese HBV S gene classification results (user:msugiyam)

job : 20110731183753

comment : FM2

query	definition	age	nearest public entry				difference between queries								nearest cluster
			ID	subtype	overlap len	mismatch	overlap len	probe0		probe1		probe2		probe3	
								N-diff	Prob	N-diff	Prob	N-diff	Prob	N-diff	Prob
probe0	Child	7	AB246345	C	250	2	244	0	1	0	1	0	1	4	0.000000e+00	AB246345
probe1	Mother, Sister1	41	AB246345	C	249	1		0	1	0	1	0	1	4	0.000000e+00	AB246345, probe0
probe2	Sister2	27	AB246345	C	248	0		0	1	0	1	0	1	4	0.000000e+00	AB246345, probe0, probe1
probe3	Sister3	30	AB222735	C	246	2		4	0.000000e+00	4	0.000000e+00	4	0.000000e+00	0	1	AB247916, AB222735

Figure 3 WWW-based user interface and the results of the matrix calculation by the software. The queries registered on the system were multi-aligned and analyzed for the calculation of mismatched nucleotides between the members of the family. This figure shows a representative result using FM2 data. The definition column presents sample information. The age column shows the point when their sera was collected. The nearest public entry shows the data locating near the query and displays the genotype, the length of query, and mismatched nucleotides compared with the nearest reference entry. The column of the difference between queries represents the mismatched nucleotides between the queries. The N-diff column shows the mismatched nucleotides between the queries. The probability value of the difference between two queries displays the prob column.

infected with HBV. These 10 families were analyzed to determine the transmission route using the present system. Predictably, two or three sequence data obtained from one family were classified into one cluster except for FM2 case (data not shown), and then the transmission routes of these nine families were intrafamilial as was expected.

A case of multiple transmission routes in a family

Interestingly, the result of FM2 case was different from the others. As shown in Table 1 and Figure 2, the family consisted of four carriers (three sisters and one of their sons). The number of nucleotide differences was calculated after the multiple-alignment by CLUSTAL W. Sample ID 6 (sister 3, S3) showed four mismatched nucleotides compared with the other members in the family (see the column of difference between queries in Fig. 3), and then the phylogenetic tree was described using E-PAS in HVDB. As shown in Figure 4, the sequence of ID 6 was classified into the cluster far from the other member, suggesting that ID 6 was infected with a different HBV clone from the other member. The probability value (abbreviated as Prob in Fig. 3) of intrafamilial transmission between two queries is displayed in the browser.

DISCUSSION

WE HAVE DEVELOPED an easy-to-use system for the calculation of phylogenetic analysis. The present system (E-PAS) was constructed for non-specialist users of genetics as well as specialists and would provide the appropriate results with several adjusted parameters by just preparing sequence data. Therefore, this system is recommended to users who want to easily investigate transmission routes of samples. In the present study, we have applied the E-PAS to the determination of transmission routes in families. Almost all of the family-cases showed intrafamilial transmission because the queries belonging to one family were classified in same cluster or a neighboring position. In the analysis between families, these queries certainly were located in the distinct cluster. One patient (sample ID 6) showed quite different sequences from the other members of her family. We did not determine whether her transmission route was vertical or horizontal as data of her parents on HBV infection were not provided. If both parents were HBV carriers, the different sequences could be detectable among ID 4, 5, and 6 as an intrafamilial transmission from father or mother to child, or she was infected by a vertical transmission from non-familial member.

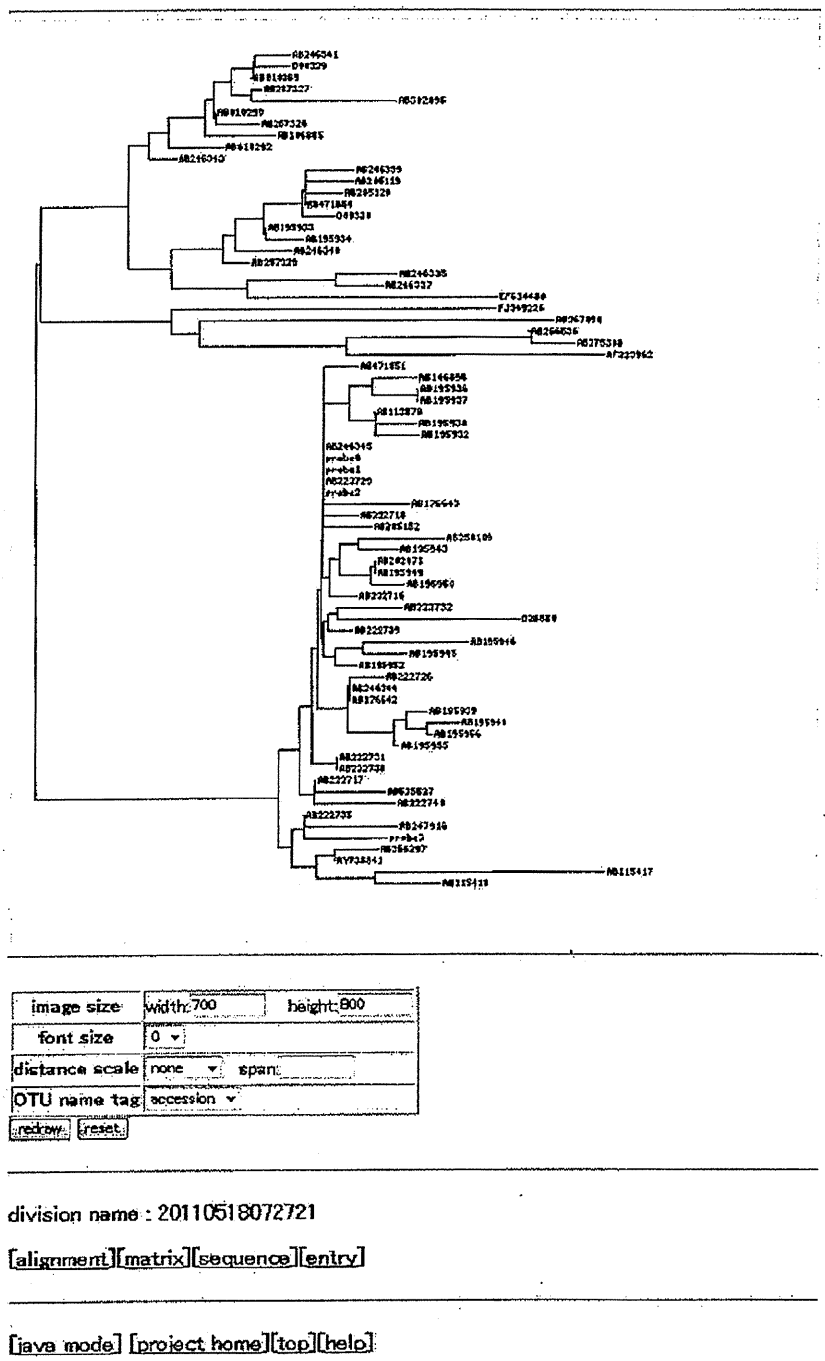

Figure 4 WWW-based user interface and the results of the phylogenetic tree. The phylogenetic tree was calculated based on the matrix data of mismatched nucleotides. A representative result using FM2 data was shown. The character in red indicates the queries. Three members of FM2 had the same sequence in the S region and were classified into the same cluster, whereas sample ID 6 (showed as probe 3 in tree) was classified into another cluster.

The primer set designed in the S region revealed high sensitive amplification because samples with low titer of HBV DNA under the limit of measurement were amplified effectively and the single band was detected in almost all samples by only the 1st PCR. Although we have estimated the substitution rate for HBV to be 4.57×10^{-5} per site per year,[27] the amplified region is a relatively highly conserved area even under antiviral drug pressure[29,30] and the region shows the genotype-dependent sequence. Therefore, a transmission route of sample ID 6 could be divided from that of the other family members. In line with this result, the determination of transmission routes and/or genotyping was achieved sufficiently even if HBV DNA was negative in conventional diagnosis. Therefore, these procedures should be determined with great caution to avoid contamination by trained researchers. The software based on a WWW-browser was customized to fit a Japanese population for quick calculation by reducing entry sequences of foreign origin. Additional datasets are under development because the present system focused on genotype B and C that are originally prevalent in Japan.

This is a versatile tool as the route of suspicious intrafamilial transmission and the genotype were determined in this assay. HBV/A has recently spread out among the young heterosexual population in addition to men who have sex with men.[16,18,19] The determination of transmission routes could contribute to epidemiological research and/or the decision of government policy to prevent the spread of HBV/A. Generally, acute hepatitis B in adulthood becomes chronic in only <1% of cases, which is much less frequent than that in Europe and the United States (approximately 10%). Since HBV/A has been more frequently observed recently in Japan, especially in metropolitan areas, HBV/A infection could provide an increased risk of chronic diseases. Further, HBV/A might be a majority of HBV infection in Japan. Reference sequence of HBV/A registered on this system could be also the appropriate reference for genotyping of HBV/A extracted from Japanese because the HBV/A2 isolates detected in Japan were homologous to those from Europe and the United States in the phylogenetic analysis.[19]

In conclusion, we have developed the easy-to-use system, E-PAS, to determine the transmission route. E-PAS separated one case infected with a clone that was different from the family, which had been expected to be intrafamilial transmission. The system is expected to accelerate the phylogenetic analysis for researchers or physicians who are not familiar with molecular genetics. Although the E-PAS has been primarily developed for Japanese patients, we are planning to extend the application for other patients by collecting foreign samples and reference sequences in addition to improve the calculation method of genetic distance.

ACKNOWLEDGMENTS

THIS WORK WAS supported by a Grant-in-Aid from the Ministry of Health Labor and Welfare of Japan and a Grant-in-Aid for JSPS Fellows of the Ministry of Education, Culture, Sports, Science, and Technology of Japan. The authors thank Professor Takashi Gojobori, National Institute of Genetics and Professor Yoshiyuki Suzuki, Nagoya City University for their professional opinion and technical support. We also thank Ms. Masako Awano, Ms. Miwa Noda, Ms. Ryuko Izumida, Ms. Mikako Kajio, and Ms. Mika Saito for their secretarial support. Laboratory work performed by Ms. Sachiko Sato, Ms. Miki Yoshida, Ms. Chieko Haga, Ms. Mami Ohashi, and Ms. Naomi Nomura is highly appreciated.

REFERENCES

1 Arauz-Ruiz P, Norder H, Robertson BH, Magnius LO. Genotype H: a new Amerindian genotype of hepatitis B virus revealed in Central America. *J Gen Virol* 2002; 83: 2059–73.
2 Chang MH. Impact of hepatitis B vaccination on hepatitis B disease and nucleic acid testing in high-prevalence populations. *J Clin Virol* 2006; 36 (Suppl 1): S45–50.
3 Chen DS. Hepatitis B vaccination: the key towards elimination and eradication of hepatitis B. *J Hepatol* 2009; 50: 805–16.
4 Kao JH, Chen DS. Global control of hepatitis B virus infection. *Lancet Infect Dis* 2002; 2: 395–403.
5 Tada H, Uga N, Fuse Y *et al.* Prevention of perinatal transmission of hepatitis B virus carrier state. *Acta Paediatr Jpn* 1992; 34: 656–9.
6 Stevens CE, Beasley RP, Tsui J, Lee WC. Vertical transmission of hepatitis B antigen in Taiwan. *N Engl J Med* 1975; 292: 771–4.
7 Sung JL, Chen DS. Maternal transmission of hepatitis B surface antigen in patients with hepatocellular carcinoma in Taiwan. *Scand J Gastroenterol* 1980; 15: 321–4.
8 Szmuness W, Prince AM, Hirsch RL, Brotman B. Familial clustering of hepatitis B infection. *N Engl J Med* 1973; 289: 1162–6.
9 Lok AS, Lai CL, Wu PC, Wong VC, Yeoh EK, Lin HJ. Hepatitis B virus infection in Chinese families in Hong Kong. *Am J Epidemiol* 1987; 126: 492–9.

10 Dumpis U, Holmes EC, Mendy M *et al.* Transmission of hepatitis B virus infection in Gambian families revealed by phylogenetic analysis. *J Hepatol* 2001; 35: 99–104.
11 Okamoto H, Tsuda F, Sakugawa H *et al.* Typing hepatitis B virus by homology in nucleotide sequence: comparison of surface antigen subtypes. *J Gen Virol* 1988; 69 (Pt 10): 2575–83.
12 Norder H, Courouce AM, Magnius LO. Complete genomes, phylogenetic relatedness, and structural proteins of six strains of the hepatitis B virus, four of which represent two new genotypes. *Virology* 1994; 198: 489–503.
13 Stuyver L, De Gendt S, Van Geyt C *et al.* A new genotype of hepatitis B virus: complete genome and phylogenetic relatedness. *J Gen Virol* 2000; 81: 67–74.
14 Orito E, Ichida T, Sakugawa H *et al.* Geographic distribution of hepatitis B virus (HBV) genotype in patients with chronic HBV infection in Japan. *Hepatology* 2001; 34: 590–4.
15 Kobayashi M, Ikeda K, Arase Y *et al.* Change of hepatitis B virus genotypes in acute and chronic infections in Japan. *J Med Virol* 2008; 80: 1880–4.
16 Yano K, Tamada Y, Yatsuhashi H *et al.* Dynamic epidemiology of acute viral hepatitis in Japan. *Intervirology* 2010; 53: 70–5.
17 Suzuki Y, Kobayashi M, Ikeda K *et al.* Persistence of acute infection with hepatitis B virus genotype A and treatment in Japan. *J Med Virol* 2005; 76: 33–9.
18 Yotsuyanagi H, Okuse C, Yasuda K *et al.* Distinct geographic distributions of hepatitis B virus genotypes in patients with acute infection in Japan. *J Med Virol* 2005; 77: 39–46.
19 Matsuura K, Tanaka Y, Hige S *et al.* Distribution of hepatitis B virus genotypes among patients with chronic infection in Japan shifting toward an increase of genotype A. *J Clin Microbiol* 2009; 47: 1476–83.
20 Mizokami M, Gojobori T, Lau JY. Molecular evolutionary virology: its application to hepatitis C virus. *Gastroenterology* 1994; 107: 1181–2.
21 Shin IT, Tanaka Y, Tateno Y, Mizokami M. Development and public release of a comprehensive hepatitis virus database. *Hepatol Res* 2008; 38: 234–43.
22 Thompson JD, Higgins DG, Gibson TJ. CLUSTAL W: improving the sensitivity of progressive multiple sequence alignment through sequence weighting, position-specific gap penalties and weight matrix choice. *Nucleic Acids Res* 1994; 22: 4673–80.
23 Gojobori T, Ishii K, Nei M. Estimation of average number of nucleotide substitutions when the rate of substitution varies with nucleotide. *J Mol Evol* 1982; 18: 414–23.
24 Saitou N, Nei M. The neighbor-joining method: a new method for reconstructing phylogenetic trees. *Mol Biol Evol* 1987; 4: 406–25.
25 Locarnini SA, Yuen L. Molecular genesis of drug-resistant and vaccine-escape HBV mutants. *Antivir Ther* 2010; 15: 451–61.
26 Zoulim F, Locarnini S. Hepatitis B virus resistance to nucleos(t)ide analogues. *Gastroenterology* 2009; 137: 1593–608 e1-2.
27 Orito E, Mizokami M, Ina Y *et al.* Host-independent evolution and a genetic classification of the hepadnavirus family based on nucleotide sequences. *Proc Natl Acad Sci USA* 1989; 86: 7059–62.
28 Osiowy C, Giles E, Tanaka Y, Mizokami M, Minuk GY. Molecular evolution of hepatitis B virus over 25 years. *J Virol* 2006; 80: 10307–14.
29 Mizokami M, Orito E, Ohba K, Ikeo K, Lau JY, Gojobori T. Constrained evolution with respect to gene overlap of hepatitis B virus. *J Mol Evol* 1997; 44 (Suppl 1): S83–90.
30 Pallier C, Castera L, Soulier A *et al.* Dynamics of hepatitis B virus resistance to lamivudine. *J Virol* 2006; 80: 643–53.

Nuclear Chk1 prevents premature mitotic entry

Makoto Matsuyama[1,2,*], Hidemasa Goto[1,3,*], Kousuke Kasahara[1,*], Yoshitaka Kawakami[4], Makoto Nakanishi[5], Tohru Kiyono[6], Naoki Goshima[4] and Masaki Inagaki[1,3,‡]

[1]Division of Biochemistry, Aichi Cancer Center Research Institute, Chikusa-ku, Nagoya 464-8681, Japan
[2]The Foundation for Promotion of Cancer Research, Chuo-ku, Tokyo 104-0045, Japan
[3]Department of Cellular Oncology, Graduate School of Medicine, Nagoya University, Showa-ku, Nagoya 466-8550, Japan
[4]Biomedicinal Information Research Center (BIRC), National Institute of Advanced Industrial Science and Technology (AIST), 2-4-7 Aomi, Koto-ku, Tokyo 135-0064, Japan
[5]Biochemistry, Nagoya City University Medical School, Nagoya, Aichi 467-8601, Japan
[6]Division of Virology, National Cancer Center Research Institute, Chuo-ku, Tokyo 104-0045, Japan
*These authors contributed equally to this work
‡Author for correspondence (minagaki@aichi-cc.jp)

Accepted 23 March 2011
Journal of Cell Science 124, 2113-2119

doi:10.1242/jcs.086488

Summary

Chk1 inhibits the premature activation of the cyclin-B1–Cdk1. However, it remains controversial whether Chk1 inhibits Cdk1 in the centrosome or in the nucleus before the G2–M transition. In this study, we examined the specificity of the mouse monoclonal anti-Chk1 antibody DCS-310, with which the centrosome was stained. Conditional Chk1 knockout in mouse embryonic fibroblasts reduced nuclear but not centrosomal staining with DCS-310. In $Chk1^{+/myc}$ human colon adenocarcinoma (DLD-1) cells, Chk1 was detected in the nucleus but not in the centrosome using an anti-Myc antibody. Through the combination of protein array and RNAi technologies, we identified Ccdc-151 as a protein that crossreacted with DCS-310 on the centrosome. Mitotic entry was delayed by expression of the Chk1 mutant that localized in the nucleus, although forced immobilization of Chk1 to the centrosome had little impact on the timing of mitotic entry. These results suggest that nuclear but not centrosomal Chk1 contributes to correct timing of mitotic entry.

Key words: Cdk1, Centrosome, Chk1, Nucleus, G2–M transition

Introduction

The cell division cycle is a tightly regulated set of events to distribute complete and accurate replicas of the genome to daughter cells. Checkpoints monitor DNA replication and repair, and thereby couple the completion of these events to the onset of mitosis. In the center of these pathways, there exists a protein kinase cascade from ataxia-telangiectasia and Rad3-related (ATR) to Chk1, the activation of which requires ssDNA and several nuclear proteins, such as replication protein A (RPA), ATR interacting protein (ATRIP), Rad9-Rad1-Hus1 (9-1-1) checkpoint complex, topoisomerase (DNA) II binding protein 1 (TOPBP1), and claspin (Zhou and Elledge, 2000; Chini and Chen, 2004; Kastan and Bartek, 2004; Cimprich and Cortez, 2008; Reinhardt and Yaffe, 2009). ATR phosphorylates Chk1 at Ser317 and Ser345, which then induces autophosphorylation of Chk1 at Ser296. These phosphorylation events are required for the transmission of checkpoint signals to downstream effectors (Zhao and Piwnica-Worms, 2001; Walker et al., 2009; Kasahara et al., 2010). With regard to the cell cycle arrest, Chk1 phosphorylates and inactivates members of the Cdc25 family of dual specificity phosphatases (Neely and Piwnica-Worms, 2003; Boutros et al., 2007). Since these enzymes control cyclin-B1–Cdk1 activation through the dephosphorylation of Thr14 and Tyr15 in the ATP-binding loop of Cdk1 (Nigg, 2001; Doree and Hunt, 2002; Nurse, 2002), activation of Chk1 eventually blocks premature mitotic entry (Lindqvist et al., 2009).

Recent studies have also demonstrated that Chk1 prevents Cdk1 from unscheduled activation even in an unperturbed cell cycle (Kramer et al., 2004; Enomoto et al., 2009). Two models were proposed to explain how Chk1 shields Cdk1 from premature activation. In one model, centrosome-associated Chk1 prevents premature activation of Cdk1 (Kramer et al., 2004; Tibelius et al., 2009). By using the anti-Chk1 monoclonal antibody DCS-310, Kramer and colleagues reported that Chk1 localized to centrosomes in interphase cells but not in prophase cells (Kramer et al., 2004). The 8-day stable induction of GFP-Chk1–PACT (pericentrin-AKAP450 centrosomal targeting domain) inhibited the G2–M transition. Based on these data, they proposed that Chk1 dissociates from the centrosome at the G2–M transition and then cyclin-B1–Cdk1 is activated on the centrosome (Kramer et al., 2004; Tibelius et al., 2009). This centrosomal model is well fit for the observation that active cyclin-B1–Cdk1 was first detected on the centrosome (Jackman et al., 2003). In the other model, nuclear Chk1 prevents premature activation of Cdk1 (Enomoto et al., 2009). By using three independent anti-Chk1 monoclonal antibodies including DCS-310, we have previously demonstrated that Chk1 translocates from the nucleus to the cytoplasm at the G2–M transition (Enomoto et al., 2009). This translocation is regulated by Cdk1-induced Chk1 phosphorylation at Ser286 and Ser301 (Shiromizu et al., 2006), and disturbance of this process results in a delay in mitotic entry (Enomoto et al., 2009). Thus, we have proposed a model in which Cdk1-induced Chk1 phosphorylation leads to the elimination of active Chk1 kinase from the nucleus, which triggers a positive feedback loop of Cdk1 activation in the nucleus. This nuclear model is fits well the observation that Chk1 activation occurs predominantly in the nucleus (Sanchez et al., 1997; Jiang et al., 2003).

The spatiotemporal regulation of several protein kinase activities is considered to have crucial roles in the coordination of

centrosomal, cytoplasmic, and nuclear events during cell cycle progression and checkpoints (Nigg, 2001; Reinhardt and Yaffe, 2009). Since the centrosome is considered to be a hub in which the cyclin-B1–Cdk1 complex is first activated (Jackman et al., 2003), the centrosomal Chk1 model is attractive. However, this centrosomal model is based largely on the use of one anti-Chk1 antibody, DCS-310 (Kramer et al., 2004; Tibelius et al., 2009). In this present study, we show that the centrosomal reactivity of this antibody reflects the crossreactivity with another protein, Cdc151, and that Chk1 does not localize to the centrosome. In addition, forced localization of Chk1 to the centrosome has little effect on the entry into mitosis, whereas forced nuclear transport caused a delay in mitotic entry.

Results and Discussion

Chk1 is localized predominantly in the nucleus but not on the centrosome

An anti-Chk1 monoclonal antibody DCS-310 is reported to react with the centrosome in cells fixed with methanol:acetone (1:1) (Kramer et al., 2004; Tibelius et al., 2009). We confirmed that DCS-310 reacts with the centrosome in cells fixed with methanol:acetone (1:1) (Fig. 1B and Fig. 3D) or 1% formaldehyde (Fig. 2E) but not with 3.7% formaldehyde (not depicted). However, especially in methanol–acetone-fixed cells (Fig. 1B and Fig. 3D), nuclear and cytoplasmic DCS-310 signals are much weaker than in cells fixed with 3.7% formaldehyde (Enomoto et al., 2009). In the experiments described here, we used cells fixed in methanol:acetone (1:1) or 1% formaldehyde to evaluate centrosomal DCS-310-staining.

We used $Chk1^{flox/-}$ mouse embryonic fibroblasts (MEFs) in which one *lox*-flanked (flox) *Chk1* allele can be converted into a null allele by Cre–*lox* site-specific homologous recombination (Niida et al., 2005) to examine the effect of conditional Chk1 knockout on the DCS-310-immunoreactivity. For this purpose, we infected $Chk1^{flox/-}$ MEFs with an adenovirus carrying either β-galactosidase (Ad-LacZ; the infection control) or Cre recombinase (Ad-Cre) as described previously (Shimada et al., 2008) and then analyzed them 3 days after the infection. As shown in Fig. 1A, we detected a 54-kDa band that corresponds to mouse Chk1 in the MEFs infected with Ad-LacZ but not with Ad-Cre, demonstrating the success of conditional Chk1 knockout. As shown in Fig. 1B, nuclear and cytoplasmic DCS-310 signals were decreased in $Chk1^{\Delta/-}$ MEFs (infected with Ad-Cre), compared with $Chk1^{flox/-}$ MEFs (infected with Ad-LacZ). However, we observed only marginal differences in the centrosomal staining between these two cells (Fig. 1B); a similar tendency was observed using MEFs fixed with 1% formaldehyde (not shown). These results suggest that, at least on the centrosome, DCS-310 crossreacts with protein(s) other than Chk1.

We next replaced one *CHK1* allele with Myc-tagged Chk1 in stable human colon adenocarcinoma (DLD-1) cells (Fig. 2). As shown in Fig. 2A, we performed homology-directed gene replacement with recombinant adeno-associated virus (rAAV) vector (Kohli et al., 2004; Rago et al., 2007). One *CHK1* allele was targeted by rAAV infection, drug selection and screening by PCR. We confirmed the isolation of heterozygotes, $Chk1^{+/myc}$ cell clones by Southern blot hybridization (Fig. 2B) and by western blotting (Fig. 2C). We treated $Chk1^{+/myc}$ cells with hydroxyurea (HU) in order to activate the DNA replication checkpoint (Fig. 2D). Like wild-type Chk1, Myc-Chk1 (lower and upper bands, respectively) was phosphorylated at Ser345 in HU-treated cells (Fig. 2D), confirming that Myc-Chk1 expressed in DLD-1 cells was functional. In $DLD\text{-}1^{+/myc}$ cells fixed with 1% formaldehyde, the nucleus was strongly stained not only by DCS-310 but also anti-

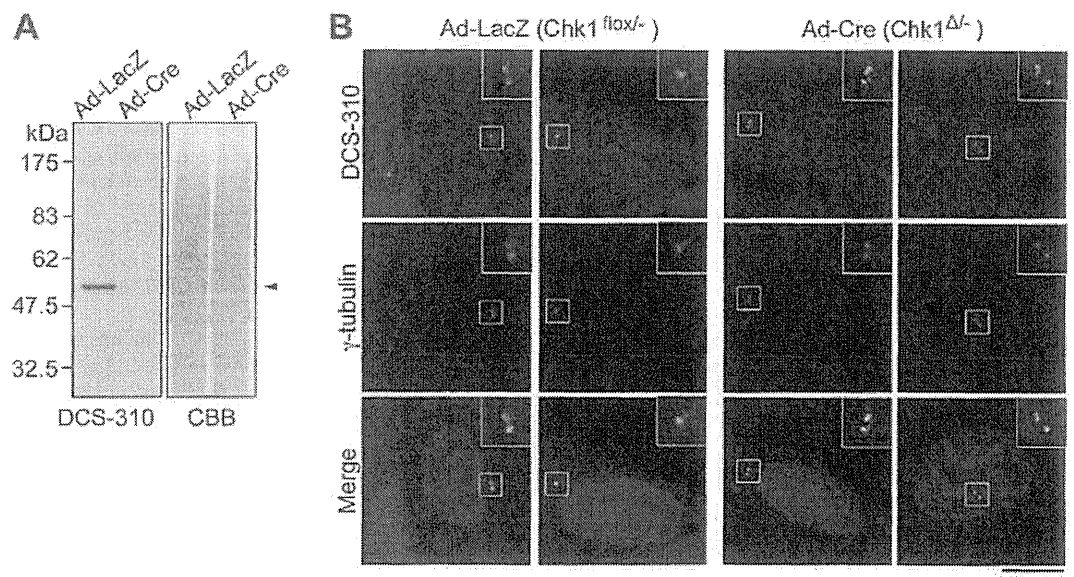

Fig. 1. The centrosome stained positive for Chk1 with the monoclonal antibody DCS-310, even after conditional Chk1 knockout. (**A**,**B**) $Chk1^{flox/-}$ MEFs (Niida et al., 2005) were infected with adenovirus carrying β-galactosidase (Ad-LacZ; infection control) or Cre recombinase (Ad-Cre), as described previously (Shimada et al., 2008). At 3 days after infection, cells were subjected to western blotting (A) or immunocytochemistry (B) with DCS-310. After blotting, transferred membrane was stained with Coomassie Brilliant Blue (CBB; A). Cells were co-stained with anti-γ-tubulin (to detect centrosomes) and DAPI (to detect nuclei; B). Boxed areas (top right) in B show the indicated centrosomes at high magnification. Scale bar: 5 μm.

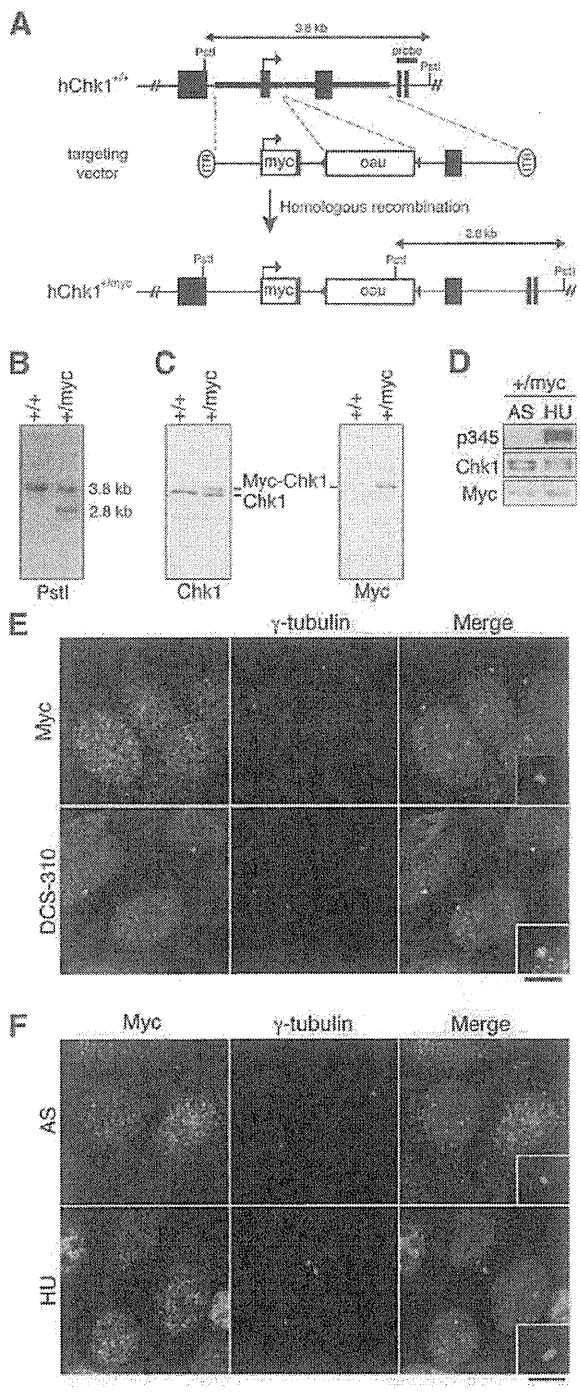

Fig. 2. Chk1 localized mainly in nucleus but not on centrosome. (**A**) Strategy of Chk1$^{+/myc}$ DLD-1 cell generation. The rAAV targeting vector contains sequences from *CHK1* locus flanking a neomycin resistance (*neo*) marker bounded by *loxP* sites. DNA sequence corresponding to Myc-epitope (amino acid sequence; EQKLISEEDL) was inserted between first ATG and the second codon on exon 2. The diagram indicates the positions of Chk1-derived sequences in the targeting vector and of the labeled hybridization probe relative to *PstI* sites. The predicted restriction map of targeted *CHK1* allele is also shown (hChk1$^{+/myc}$). (**B**,**C**) Established heterozygotes (+/myc) were subjected to Southern (B) and western (C) blot analyses. The Southern blot hybridization to *PstI*-digested genomic DNA shows single band of ~3.8 kb in wild-type (+/+) and two bands of ~3.8 kb and ~2.8 kb with similar intensity in heterozygotes (+/myc). Positions of Myc-tagged Chk1 (Myc-Chk1) and wild-type Chk1 (Chk1) are indicated (C). (**D**) Chk1$^{+/myc}$ DLD-1 cells were treated with 3 mM hydroxyurea (HU) or left untreated (AS) for 16 hours. Then, cells were subjected to western blotting with indicated antibodies. (**E**,**F**) Chk1$^{+/myc}$ DLD-1 cells were subjected to immunocytochemistry with anti-Myc or DCS-310, together with anti-γ-tubulin and DAPI. HU treatment was performed as described above. Scale bars: 5 μm.

Myc antibody (Fig. 2E). However, unlike DCS-310, the centrosome was hardly stained by anti-Myc antibody (Fig. 2E). Since Chk1 had been reported to accumulate in the nucleus (Sanchez et al., 1997; Jiang et al., 2003) or on the centrosome (Loffler et al., 2007; Niida et al., 2007) in response to the checkpoint activation, we also stained HU-treated Chk1$^{+/myc}$ cells with anti-Myc antibody. Regardless of the HU treatment, we hardly detected anti-Myc signals on the centrosome (Fig. 2F). However, HU treatment enhanced nuclear Myc signals (Fig. 2F). Since these signals were detected only at low or background levels in parental (Chk1$^{+/+}$) DLD-1 cells (supplementary material Fig. S1), the majority of observed Myc signals in Chk1$^{+/myc}$ cells reflected the staining of Myc-tagged Chk1 but not of endogenous Myc. Thus, these results suggest that Chk1 is localized predominantly in the nucleus but not on the centrosome.

We then searched for DCS-310-reactive centrosomal protein(s) using a protein array system (Goshima et al., 2008). Among 19,900 proteins, we identified 18 proteins (including Chk1) as being DCS-310-reactive (supplementary material Fig. S2 and Table S1). In order to examine which protein(s) localize to the centrosome, we introduced each Flag-tagged protein into HeLa cells. As shown in Fig. 3A,B (also see supplementary material Fig. S3), two independent proteins, bicaudal D homolog 2 (Bicd2) (Splinter et al., 2010) and the non-characterized protein coiled-coil domain containing 151 (Ccdc151), were validated as candidate centrosomal proteins, although Flag-tagged Chk1 was localized predominantly in the nucleus but not on the centrosome. RNA interference (RNAi) experiments showed that depletion of Ccdc151 specifically reduced DCS-310 immunoreactitity on the centrosome (Fig. 3C,D). All these results suggest that centrosomal DCS-310 immunoreactivity reflects the existence of Ccdc151 but not Chk1 on the centrosome.

Nuclear but not centrosomal Chk1 prevents Cdk1 from premature activation

For functional analyses of Chk1, we established Tet-On HeLa cells in which each type of Myc-tagged Chk1 (Myc-Chk1) is expressed in a doxycycline (Dox)-dependent manner. After the addition of 0.3 μg/ml Dox, the expression level of Myc-Chk1 fused to PACT (Myc-Chk1–PACT) was comparable to that of Myc-Chk1 wild-type (WT), Chk1 kinase-inactive mutant (K38M) or of a mutant in which two serine phosphorylation sites of Cdk1 were changed to alanine (S286/301A) (Fig. 4A). Under this condition, Myc-Chk1–PACT localized predominantly on the centrosome, whereas other types of Myc-Chk1 mutant were localized predominantly in the nucleus but not on the centrosome (Fig. 4B). We next evaluated the effect of each protein expression on the G2–M transition and cyclin-B1–Cdk1 activation in the following method (summarized in Fig. 4C). As shown in Fig. 4D, each Tet-On cell line was synchronized at the G1–S boundary by the double-thymidine block

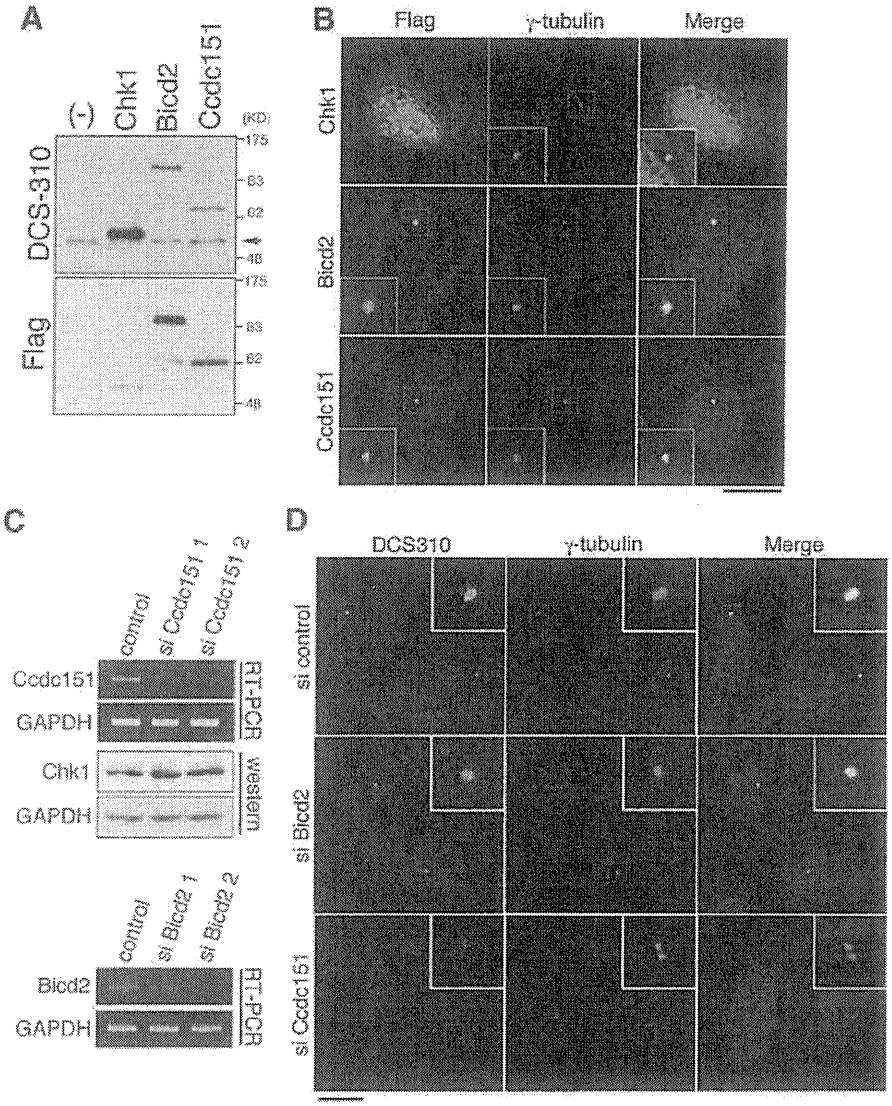

Fig. 3. Centrosomal staining of anti-Chk1 antibody DCS-310 indicates the presence of Ccdc151 but not Chk1 on centrosomes. (A,B) HeLa cells were transfected with pDEST12.2 (Invitrogen) each carrying a Flag-tagged protein. As a negative control, we used pDEST12.2 carrying only Flag ( ). After transfection, cells were subjected to western blotting (A) or immunocytochemistry (B). The arrowhead in A indicates the position of endogenous Chk1. (C,D) HeLa cells were transfected with siRNA as indicated. At 72 hours after transfection, cells were subjected to RT-PCR, western blotting (C) or immunocytochemistry (D). Since we observed only marginal differences in immunocytochemistry between two sequences targeted to each protein (not depicted), data by using one target sequence are indicated (D). Scale bars: 5 μm.

(DTB) method. At the release of the second thymidine block, we added 0.3 μg/ml Dox to the growing medium for the induction of each Myc-Chk1. From 6–13 hours after the release, cells were collected and then subjected to immunocytochemistry (to evaluate mitotic index; Fig. 4F) or in-vitro H1 kinase assays by using anti-Cyclin B1 immunocomplex (to evaluate the activity of cyclin-B1–Cdk1 complex; Fig. 4G). Without Dox addition (Myc-Chk1 induction), we observed only marginal changes in the timing of mitotic entry among the established cell lines (Fig. 4E). WT expression delayed the timing not only of mitotic entry (Fig. 4F) but also of cyclin-B1–Cdk1 activation (Fig. 4G), compared with the K38M mutant. The timing was more delayed when mutant S286/301A was expressed (Fig. 4F,G), confirming the existence of a positive feedback loop between Cdk1 and Chk1 (Enomoto et al., 2009). However, we observed only marginal effects when Myc-Chk1–PACT was expressed, similar to the experiments with the K38M mutant (Fig. 4F,G). These results suggest that forced immobilization of Chk1 to the centrosome has little impact on the timing of mitotic entry and activation of Cdk1.

These observations appeared to contrast with the previous report that stable induction of GFP-Chk1–PACT inhibited the G2–M transition. We consider that this discrepancy might be partly caused by the difference in the expression level of Chk1–PACT. In the case of higher expression of Myc-Chk1–PACT (by use of 1–2 μg/ml Dox), Myc-Chk1–PACT was not restricted to the centrosome; it also localized to the nucleus (Fig. 4H,I). Under this condition, the expression of Myc-Chk1–PACT also delayed the timing of mitotic entry, like WT expression (Fig. 4J). These results imply one possibility, namely that the localization of mutant Chk1–PACT is highly dependent on its level of expression and that reflects the phenotype.

We also evaluated the effect of the expression of Myc-Chk1 WT with three repeated sequences of NLS at the C-terminus (Myc-Chk1-3×NLS). The expression level of Myc-Chk1-3×NLS was

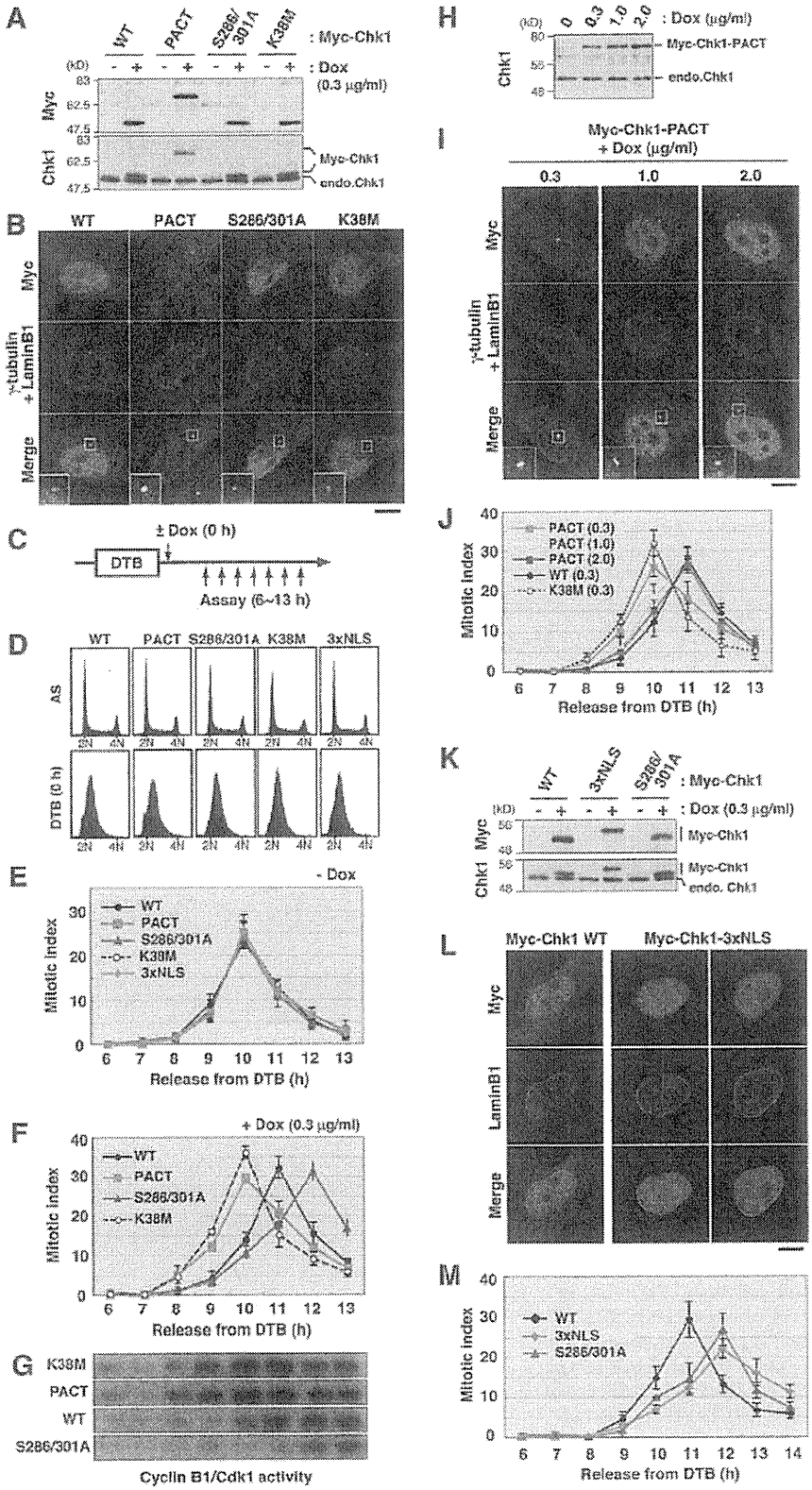

Fig. 4. Nuclear but not centrosomal Chk1 prevents Cdk1 from unscheduled activation. (A–M) Each Tet-ON cell line was incubated with (+) or without (–) doxycycline (Dox) for 16 hours after which the cells were subjected to western blotting (A,H,K) or immunocytochemistry (B,I,L). Positions of endogenous Chk1 (endo. Chk1) or exogenous Myc-Chk1 are indicated (A,H,K). Cells were co-stained with anti-γ-tubulin (B,I) and anti-lamin-B1 (to detect nuclear membrane; B,I,L). To evaluate the effect of each Myc-Chk1 expression on mitotic entry (F,J,M) and Cdk1 activity (G), the following experiments were performed as indicated (C). Each Tet-On cell line was synchronized at the G1–S boundary using the double thymidine block (DTB) method. To confirm the synchrony of each cell line by DTB, some cells were subjected to FACS analyses (Time 0; D). As a control, FACS analyses were also performed using random culture cells (AS; D). Upon release of second thymidine block, Dox was added to the growth medium to induce Myc-Chk1. Between 6 hours and 13 hours after release, cells were collected and subjected to immunocytochemistry (F,J,M) or in vitro H1 kinase assays using anti-Cyclin B1 immunocomplex (G). As a control, the timing of mitotic entry without Myc-Chk1 induction was analyzed (Dox addition; E). Plotted data of mitotic indices at each time point represent mean ± s.e.m. of 200 cells from three independent experiments (E,F,J,M). Cyclin-B1–Cdk1 activity in each sample was visualized through autoradiography of H1 (G). Scale bars: 10 μm.

comparable to that of Myc-Chk1 WT or mutant Chk1 S286/301A (Fig. 4K). Myc-Chk1-3×NLS was localized at higher levels than Myc-Chk1 WT in the nucleus (Fig. 4L). Like that of S286/301A, the expression of Myc-Chk1-3×NLS delayed mitotic entry more than the expression of Myc-Chk1 WT (Fig. 4M). Since the S286/301A mutant was localized predominantly in the nucleus even during the first mitotic phase prophase (Enomoto et al., 2009), all these observations suggest that nuclear Chk1 prevents Cdk1 from unscheduled activation before the G2–M transition.

In this study, we demonstrate that Chk1, when localized in the nucleus but not on the centrosome, inhibits premature Cdk1 activation. Together with our previous study (Enomoto et al., 2009), our findings here strongly support a model according to which the ATR-Chk1 pathway monitors the integrity of genomic DNA in the nucleus before mitosis. In support of this notion, all known regulators of this pathway are localized in the nucleus (see Introduction) and Chk1 accumulates in the nucleus in response to the checkpoint activation (Sanchez et al., 1997; Jiang et al., 2003). Since Chk1 did not translocate to the centrosome even in HU-treated cells (Fig. 2F), Chk1 did not directly inhibit centrosomal cyclin-B1–Cdk1 activation, which was first detected at the G2–M transition (Jackman et al., 2003). Accumulating data has demonstrated a new checkpoint pathway mediated by MAPK (p38) and MAPK-activated protein kinase-2 (MAPKAP kinase-2; MK2) that operates parallel to Chk1 and is activated downstream of ataxia telangiectasia mutated (ATM) and ATR (Bulavin et al., 2001; Manke et al., 2005; Raman et al., 2007; Reinhardt et al., 2007; Reinhardt and Yaffe, 2009). A recent study also revealed that Chk1 controls nuclear events but that the p38–MK2 pathway regulates cytoplasmic events in checkpoint responses (Reinhardt et al., 2010). Interestingly, p38 has been reported to phosphorylate and inhibit Cdc25B (Bulavin et al., 2001), which was proposed to function as a centrosomal Cdc25 (Gabrielli et al., 1996; Karlsson et al., 1999; De Souza et al., 2000; Lindqvist et al., 2005). Therefore, the p38–MK2 pathway is likely to transmit nuclear checkpoint signals generated by Chk1 to other cellular components such as the centrosome.

Our present study documents the importance of spatiotemporally regulated localization of Chk1 in the mitotic entry and paves the way for future studies that evaluate the coordination of centrosomal, cytoplasmic, and nuclear events during the checkpoint response.

Materials and Methods

Generation of the Chk1$^{+/myc}$ DLD-1 and HeLa Tet-On cell lines

The colon adenocarcinoma (DLD-1) cell line was purchased from ATCC (#CCL-221). For the construction of targeting vectors, genomic regions of the *CHK1* locus were amplified from DLD-1 genomic DNA by using primers of 5′ and 3′ homology arms. Then, site-directed mutagenesis (Stratagene, La Jolla, CA) was performed for the addition of a DNA sequence corresponding to Myc epitope (amino acid sequence; EQKLISEEDL). As shown in Fig. 2A, both homology arms and *loxP–neo–loxP* were ligated into the pAAV-MCS vector. Recombinant adeno-associated viruses (rAAVs) were produced according to the manufacturer's protocol (Stratagene). Chk1$^{+/myc}$ DLD-1 cells were established as described previously (Kohli et al., 2004; Rago et al., 2007). Each HeLa Tet-On cell line was generated as reported previously (Ikegami et al., 2008; Enomoto et al., 2009).

Transfection

For the expression of 18 DCS-310-reactive proteins in HeLa cells, pDEST12.2 carrying each Flag-tagged protein was constructed through the homologous recombination between pDEST12.2 and 'FLJ' cDNA clones (Goshima et al., 2008) using Gateway technology (Invitrogen, Carlsbad, CA). Transfection was performed with Lipofectamine™ reagent (Invitrogen) according to the manufacturer's protocol.

All small interfering RNA (siRNA) duplexes were purchased from QIAGEN (Valencia, CA). Target sequences were as follows: Bicd2 siRNAs, 5′-GGAGCUGU-CACACUACAUG-3′ (sequence 1) and 5′-GGUGGACUAUGAGGCUAUC-3′ (sequence 2) (Splinter et al., 2010); Ccdc151 siRNAs, 5′-GGAGACUAAGGCACUG-GAA-3′ (sequence 1) and 5′-CAA GGCCUAUCUAAUGGACGA-3′ (sequence 2); and non-silencing siRNA (as a negative control), 5′-UUCUCCGAACGUGUCACGU-3′. Transfection was performed with a mixture of each siRNA (final concentration 25 nM) and Lipofectamine™ RNAiMAX reagent (Invitrogen) according to the transfection procedure.

Antibodies

Antibodies against the following proteins or tags were used in the study: Chk1 (DCS310), γ-tubulin (GTU-88), Flag (M2; Sigma, St Louis, MO); Chk1 phospho-Ser345 (133D3), Myc (9B11; Cell Signaling Technology, Beverly, MA); CyclinB1 (GNS-1; BD Transduction Laboratories, San Diego, CA); rabbit laminB1, GAPDH conjugated to HRP (Abcam, Cambridge, UK).

Immunocytochemistry

Before fixation, cells were grown on glass coverslips. For immunostaining with DCS-310 (except that shown in Fig. 2) or anti-Flag, cells were fixed in –20°C methanol/acetone (1:1) for 7 minutes as described previously (Kramer et al., 2004). In other experiments, cells were treated with 1% (Fig. 2) or 3.7% (Fig. 4) formaldehyde in phosphate-buffered saline (PBS) at room temperature for 10 minutes and then with –20°C methanol for 10 minutes. Cells were incubated with primary antibodies for 1 hour and then with appropriate Alexa-Fluor-conjugated secondary antibodies (Invitrogen) for 30 minutes at room temperature. DNA was also stained with 0.5 μg/ml DAPI for 5 minutes. Each fluorescence image was captured as a single optical section using a Zeiss LSM510 confocal laser-scanning microscope (Carl Zeiss, Thornwood, NY).

In vitro H1 kinase assays using anti-Cyclin B1 immunocomplex

The cyclin-B1–Cdk1 complex was purified as an anti-cyclin-B1 immunocomplex as described previously (Ikegami et al., 2008; Enomoto et al., 2009). This immunocomplex was incubated with histone H1 as described previously (Kasahara et al., 2010). Cyclin-B1–Cdk1 activity in each sample was visualized through the autoradiography of histone H1.

Reverse-transcriptase PCR

Reverse-transcriptase (RT)-PCR was performed using the following primers as described previously (Goto et al., 2006): Ccdc151, 5′-CAGGAGAC-CATCAGTCAGCTC-3′ (forward) and 5′-GCAGGTACACGCTGGTAATGT-3′ (reverse); Bicd2, 5′-ACTCGGAGATGAGTGCTTTGA-3′ (forward) and 5′-CACAACGTCCTAAAACCCAGA-3′ (reverse); and GAPDH, 5′-GGCATGGC-CTTCCGTGTTCCT-3′ (forward) and 5′-TCCTTGCTGGGGTGGGTGGTC-3′ (reverse).

FACS analysis

For fluorescence-activated cell sorting (FACS) analysis that shows the DNA content in each group, ~10^6 treated cells were collected by trypsinization, resuspended in buffer solution (CycleTEST™ PLUS kit; Becton-Dickinson, San Diego, CA) and stored at –80°C. Then, we treated cells according to the manufacturer's protocol (CycleTEST™ PLUS kit) and analyzed them using a Becton-Dickinson FacsScan and CellQuest software.

We thank M. Shimada (Nagoya City University) and M. Enomoto (Kobe University) for preparing materials. We are also grateful to T. Kanda for the support of FACS analyses, E. Kawamoto, K. Kobori, C. Yuhara and Y. Hayashi for technical assistance, to Y. Takada for secretarial expertise, and J. Shields for critical comments on the manuscript. This work was supported in part by Grants-in-Aid for Scientific Research from the Japan Society for the Promotion of Science and from the Ministry of Education, Science, Technology, Sports and Culture of Japan; a Grant-in-Aid for the Third-Term Comprehensive 10-Year Strategy for Cancer Control from the Ministry of Health and Welfare, Japan; the Uehara Memorial Foundation; the Astellas Foundation for Research on Metabolic Disorders; the Naito Foundation; the Daiichi-Sankyo Foundation of Life Science; and by a Research Grant from the Princess Takamatsu Cancer Research Fund.

Supplementary material available online at
http://jcs.biologists.org/cgi/content/full/124/13/2113/DC1

References

Boutros, R., Lobjois, V. and Ducommun, B. (2007). CDC25 phosphatases in cancer cells: key players? Good targets? *Nat. Rev. Cancer* 7, 495-507.

Bulavin, D. V., Higashimoto, Y., Popoff, I. J., Gaarde, W. A., Basrur, V., Potapova, O., Appella, E. and Fornace, A. J., Jr (2001). Initiation of a G2/M checkpoint after ultraviolet radiation requires p38 kinase. *Nature* 411, 102-107.

Chini, C. C. and Chen, J. (2004). Claspin, a regulator of Chk1 in DNA replication stress pathway. *DNA Repair* 3, 1033-1037.

Cimprich, K. A. and Cortez, D. (2008). ATR: an essential regulator of genome integrity. *Nat. Rev.* 9, 616-627.

De Souza, C. P., Ellem, K. A. and Gabrielli, B. G. (2000). Centrosomal and cytoplasmic Cdc2/cyclin B1 activation precedes nuclear mitotic events. *Exp. Cell Res.* 257, 11-21.

Doree, M. and Hunt, T. (2002). From Cdc2 to Cdk1: when did the cell cycle kinase join its cyclin partner? *J. Cell Sci.* 115, 2461-2464.

Enomoto, M., Goto, H., Tomono, Y., Kasahara, K., Tsujimura, K., Kiyono, T. and Inagaki, M. (2009). Novel positive feedback loop between Cdk1 and Chk1 in the nucleus during G2/M transition. *J. Biol. Chem.* 284, 34223-34230.

Gabrielli, B. G., De Souza, C. P., Tonks, I. D., Clark, J. M., Hayward, N. K. and Ellem, K. A. (1996). Cytoplasmic accumulation of cdc25B phosphatase in mitosis triggers centrosomal microtubule nucleation in HeLa cells. *J. Cell Sci.* 109, 1081-1093.

Goshima, N., Kawamura, Y., Fukumoto, A., Miura, A., Honma, R., Satoh, R., Wakamatsu, A., Yamamoto, J., Kimura, K., Nishikawa, T. et al. (2008). Human protein factory for converting the transcriptome into an in vitro-expressed proteome. *Nat. Methods* 5, 1011-1017.

Goto, H., Kiyono, T., Tomono, Y., Kawajiri, A., Urano, T., Furukawa, K., Nigg, E. A. and Inagaki, M. (2006). Complex formation of Plk1 and INCENP required for metaphase-anaphase transition. *Nat. Cell Biol.* 8, 180-187.

Ikegami, Y., Goto, H., Kiyono, T., Enomoto, M., Kasahara, K., Tomono, Y., Tozawa, K., Morita, A., Kohri, K. and Inagaki, M. (2008). Chk1 phosphorylation at Ser286 and Ser301 occurs with both stalled DNA replication and damage checkpoint stimulation. *Biochem. Biophys. Res. Commun.* 377, 1227-1231.

Jackman, M., Lindon, C., Nigg, E. A. and Pines, J. (2003). Active cyclin B1-Cdk1 first appears on centrosomes in prophase *Nat. Cell Biol.* 5, 143-148.

Jiang, K., Pereira, E., Maxfield, M., Russell, B., Goudelock, D. M. and Sanchez, Y. (2003). Regulation of Chk1 includes chromatin association and 14-3-3 binding following phosphorylation on Ser-345. *J. Biol. Chem.* 278, 25207-25217.

Karlsson, C., Katich, S., Hagting, A., Hoffmann, I. and Pines, J. (1999). Cdc25B and Cdc25C differ markedly in their properties as initiators of mitosis. *J. Cell Biol.* 146, 573-584.

Kasahara, K., Goto, H., Enomoto, M., Tomono, Y., Kiyono, T. and Inagaki, M. (2010). 14-3-3gamma mediates Cdc25A proteolysis to block premature mitotic entry after DNA damage. *EMBO J.* 29, 2802-2812.

Kastan, M. B. and Bartek, J. (2004). Cell-cycle checkpoints and cancer. *Nature* 432, 316-323.

Kohli, M., Rago, C., Lengauer, C., Kinzler, K. W. and Vogelstein, B. (2004). Facile methods for generating human somatic cell gene knockouts using recombinant adeno-associated viruses. *Nucleic Acids Res.* 32, e3.

Kramer, A., Mailand, N., Lukas, C., Syljuasen, R. G., Wilkinson, C. J., Nigg, E. A., Bartek, J. and Lukas, J. (2004). Centrosome-associated Chk1 prevents premature activation of cyclin-B-Cdk1 kinase. *Nat. Cell Biol.* 6, 884-891.

Lindqvist, A., Kallstrom, H., Lundgren, A., Barsoum, E. and Rosenthal, C. K. (2005). Cdc25B cooperates with Cdc25A to induce mitosis but has a unique role in activating cyclin B1-Cdk1 at the centrosome. *J. Cell Biol.* 171, 35-45.

Lindqvist, A., Rodriguez-Bravo, V. and Medema, R. H. (2009). The decision to enter mitosis: feedback and redundancy in the mitotic entry network. *J. Cell Biol.* 185, 193-202.

Loffler, H., Bochtler, T., Fritz, B., Tews, B., Ho, A. D., Lukas, J., Bartek, J. and Kramer, A. (2007). DNA damage-induced accumulation of centrosomal Chk1 contributes to its checkpoint function. *Cell Cycle* 6, 2541-2548.

Manke, I. A., Nguyen, A., Lim, D., Stewart, M. Q., Elia, A. E. and Yaffe, M. B. (2005). MAPKAP kinase-2 is a cell cycle checkpoint kinase that regulates the G2/M transition and S phase progression in response to UV irradiation. *Mol. Cell* 17, 37-48.

Neely, K. E. and Piwnica-Worms, H. (2003). Cdc25A regulation: to destroy or not to destroy-is that the only question? *Cell Cycle* 2, 455-457.

Nigg, E. A. (2001). Mitotic kinases as regulators of cell division and its checkpoints. *Nat. Rev. Mol. Cell Biol.* 2, 21-32.

Niida, H., Tsuge, S., Katsuno, Y., Konishi, A., Takeda, N. and Nakanishi, M. (2005). Depletion of Chk1 leads to premature activation of Cdc2-cyclin B and mitotic catastrophe. *J. Biol. Chem.* 280, 39246-39252.

Niida, H., Katsuno, Y., Banerjee, B., Hande, M. P. and Nakanishi, M. (2007). Specific role of Chk1 phosphorylations in cell survival and checkpoint activation. *Mol. Cell. Biol.* 27, 2572-2581.

Nurse, P. (2002). Cyclin dependent kinases and cell cycle control (Nobel lecture). *Chembiochem* 3, 596-603.

Rago, C., Vogelstein, B. and Bunz, F. (2007). Genetic knockouts and knockins in human somatic cells. *Nat. Protoc.* 2, 2734-2746.

Raman, M., Earnest, S., Zhang, K., Zhao, Y. and Cobb, M. H. (2007). TAO kinases mediate activation of p38 in response to DNA damage. *EMBO J* 26, 2005-2014.

Reinhardt, H. C. and Yaffe, M. B. (2009). Kinases that control the cell cycle in response to DNA damage: Chk1, Chk2, and MK2. *Curr. Opin. Cell Biol.* 21, 245-255.

Reinhardt, H. C., Aslanian, A. S., Lees, J. A. and Yaffe, M. B. (2007). p53-deficient cells rely on ATM- and ATR-mediated checkpoint signaling through the p38MAPK/MK2 pathway for survival after DNA damage. *Cancer Cell* 11, 175-189.

Reinhardt, H. C., Hasskamp, P., Schmedding, I., Morandell, S., van Vugt, M. A., Wang, X., Linding, R., Ong, S. E., Weaver, D., Carr, S. A. et al. (2010). DNA damage activates a spatially distinct late cytoplasmic cell-cycle checkpoint network controlled by MK2-mediated RNA stabilization. *Mol. Cell* 40, 34-49.

Sanchez, Y., Wong, C., Thoma, R. S., Richman, R., Wu, Z., Piwnica-Worms, H. and Elledge, S. J. (1997). Conservation of the Chk1 checkpoint pathway in mammals: linkage of DNA damage to Cdk regulation through Cdc25. *Science* 277, 1497-1501.

Shimada, M., Niida, H., Zineldeen, D. H., Tagami, H., Tanaka, M., Saito, H. and Nakanishi, M. (2008). Chk1 is a histone H3 threonine 11 kinase that regulates DNA damage-induced transcriptional repression. *Cell* 132, 221-232.

Shiromizu, T., Goto, H., Tomono, Y., Bartek, J., Totsukawa, G., Inoko, A., Nakanishi, M., Matsumura, F. and Inagaki, M. (2006). Regulation of mitotic function of Chk1 through phosphorylation at novel sites by cyclin-dependent kinase 1 (Cdk1). *Genes Cells* 11, 477-485.

Splinter, D., Tanenbaum, M. E., Lindqvist, A., Jaarsma, D., Flotho, A., Yu, K. L., Grigoriev, I., Engelsma, D., Haasdijk, E. D., Keijzer, N. et al. (2010). Bicaudal D2, dynein, and kinesin-1 associate with nuclear pore complexes and regulate centrosome and nuclear positioning during mitotic entry. *PLoS Biol.* 8, e1000350.

Tibelius, A., Marhold, J., Zentgraf, H., Heilig, C. E., Neitzel, H., Ducommun, B., Rauch, A., Ho, A. D., Bartek, J. and Kramer, A. (2009). Microcephalin and pericentrin regulate mitotic entry via centrosome-associated Chk1. *J. Cell Biol.* 185, 1149-1157.

Walker, M., Black, E. J., Oehler, V., Gillespie, D. A. and Scott, M. T. (2009). Chk1 C-terminal regulatory phosphorylation mediates checkpoint activation by de-repression of Chk1 catalytic activity. *Oncogene* 28, 2314-2323.

Zhao, H. and Piwnica-Worms, H. (2001). ATR-mediated checkpoint pathways regulate phosphorylation and activation of human Chk1. *Mol. Cell. Biol.* 21, 4129-4139.

Zhou, B. B. and Elledge, S. J. (2000). The DNA damage response: putting checkpoints in perspective. *Nature* 408, 433-439.

Journal of Cell Science

Human Reproduction, Vol.26, No.5 pp. 1259–1266, 2011
Advanced Access publication on February 26, 2011 doi:10.1093/humrep/der035

human reproduction **ORIGINAL ARTICLE** ***Reproductive genetics***

SYCP3 mutation may not be associated with recurrent miscarriage caused by aneuploidy

Eita Mizutani [1], Nobuhiro Suzumori [1,*], Yasuhiko Ozaki [1], Kumiko Oseto [1], Chisato Yamada-Namikawa [2], Makoto Nakanishi [2], and Mayumi Sugiura-Ogasawara [1]

[1]Department of Obstetrics & Gynecology, Nagoya City University Graduate School of Medicine, 1 Kawasumi, Mizuho-cho, Mizuho-ku, Nagoya 467-8601, Japan [2]Department of Biochemistry II, Nagoya City University Graduate School of Medicine, 1 Kawasumi, Mizuho-cho, Mizuho-ku, Nagoya 467-8601, Japan

*Correspondence address. Tel: +81-52-853-8241; Fax: +81-52-842-2269; E-mail: og.n.suz@med.nagoya-cu.ac.jp

Submitted on December 4, 2010; resubmitted on January 12, 2011; accepted on January 19, 2011

BACKGROUND: *SYCP3* mutations have been shown to generate an aberrant synaptonemal complex in a dominant-negative manner and to contribute to abnormal chromosomal behavior that might lead to recurrent miscarriage. We examined whether *SYCP3* mutation is associated with recurrent miscarriage caused by embryonic aneuploidy.

METHODS: The *SYCP3* 657T>C mutation was examined using PCR and sequencing in 101 patients with a history of three or more unexplained recurrent miscarriages and 82 fertile controls with no history of miscarriage. The embryonic karyotype in the aborted conceptus was analyzed.

RESULTS: The 657T>C mutation of *SYCP3* was identified in one patient with a history of six recurrent miscarriages with embryonic euploidy and one fertile woman in the control group. Patients with abnormal and normal chromosome were found to repeat miscarriage with abnormal and normal chromosome, respectively.

CONCLUSIONS: The 657T>C mutation of *SYCP3* may not be associated with recurrent miscarriage caused by aneuploidy. We found no clinical significance of routine examination of the *SYCP3* mutation because only one benign mutation was ascertained in 101 patients.

Key words: SYCP3 / recurrent miscarriage / fetal chromosome / meiosis / polymorphism

Introduction

SYCP3 mutations in women were found to generate an aberrant synaptonemal complex in a dominant-negative manner and to contribute to abnormal chromosomal behavior that might lead to recurrent miscarriage (Bolor *et al.*, 2009). Bolor *et al.* (2009) found *SYCP3* mutations in 2 of 26 (7.7%) patients with recurrent miscarriage. SYCP3 is a DNA-binding protein and a structural component of the synaptonemal complex, which mediates the synapsis or homologous pairing of chromosomes during meiosis of the germ cells. Male mice homozygous for the null mutation of the *Sycp3* gene are sterile as a result of massive apoptotic cell death in the testis during meiotic prophase (Yuan *et al.*, 2000). *Sycp3*-deficient female mice are subfertile with a severely reduced oocyte pool. Although two-thirds of mouse offspring are healthy, one-third is affected by aneuploidy and succumbs during development *in utero* (Yuan *et al.*, 2002). This is consistent with the observations that in humans, a mutation in *SYCP3* was identified in two patients with azoospermia (Miyamoto *et al.*, 2003), and that the lack of *SYCP3* gene expression in human testis may have a negative effect on spermatogenesis and male fertility (Aarabi *et al.*, 2006).

The identifiable causes of recurrent miscarriage may include abnormal chromosomes in either partner (particularly translocations), antiphospholipid antibodies (aPL) and uterine anomalies (Farquharson *et al.*, 1984; Sugiura-Ogasawara *et al.*, 2004, 2010). A currently prevailing hypothesis is that recurrent miscarriage may be a polygenetic disorder associated with both genetic and environmental determinants. Polymorphisms related to thrombophilia, such as Leiden mutation and prothrombin mutation, are known to be associated with recurrent miscarriage, although the mutations are not found in the Asian population (Nelen *et al.*, 1996; Rey *et al.*, 2003; Rai and Regan, 2006; Suzumori and Sugiura-Ogasawara, 2010). However, whether Factor V Leiden and Factor II prothrombin polymorphisms are risk factors for recurrent miscarriage is controversial (Coulam *et al.*, 2006; Goodman *et al.*, 2006).

An abnormal embryonic karyotype causes not only sporadic spontaneous abortion but also recurrent miscarriage because it was found in 51% of recurrent cases (Ogasawara et al., 2000; Carp et al., 2001). Bolor et al. (2009) could not prove an association between the *SYCP3* mutations found in 7.7% of patients and embryonic aneuploidy.

Preimplantation genetic screening (PGS) for aneuploidy has been performed widely; however, there is no evidence of its ability to improve delivery rates (Platteau et al., 2005; The ACOG., 2009; Harper et al., 2010). The *SYCP3* mutation might be a candidate for selection of cases for PGS if an association between the mutation and aneuploidy is established. Also, the 7.7% frequency of *SYCP3* mutation is relatively high because the frequency of translocations, aPL and major uterine anomalies is 4.5% (Sugiura-Ogasawara et al., 2004), 10.7% (Balasch et al.,1990) and 3.2% (Sugiura-Ogasawara et al., 2010), respectively. Here we investigate whether *SYCP3* mutations may be associated with recurrent miscarriage caused by aneuploidy.

Materials and Methods

Patients

All patients underwent a systematic examination, including hysterosalpingography, chromosome analysis for both partners, determination of aPL, including lupus anticoagulant and β2glycoprotein I-dependent anticardiolipin antibodies (Ogasawara et al., 1996), and blood tests for hyperthyroidism, diabetes mellitus and hyperprolactinemia before subsequent pregnancy in Nagoya City University Hospital between 2007 and 2010. A blood sample was taken at the examination and frozen at −70°C before analysis. Patients with identifiable causes of miscarriage, such as translocations, aPL and uterine anomalies, were excluded. The 81 patients for whom a previous or subsequent embryonic (or fetal) karyotype was ascertained at least one time were studied. A further 20 patients for whom the embryonic karyotype was unknown were added.

In Japan, miscarriage is defined as loss within 22 weeks gestation and stillbirth is defined as loss at 22 or more weeks of gestation. Stillbirths after 22 weeks gestation were included in the present study and shown as prior history in Table I.

A total of 101 patients with a history of three or more (3–16) unexplained consecutive first-trimester miscarriages were examined. Subsequent pregnancies were followed up until October 2010. The mean age of participants at examination was 34.4 ± 3.8 years, and the average number of previous miscarriages was 3.8 ± 2.7. Twenty-four patients had a history of live birth and two patients experienced recurrent miscarriage after changing partner, having had a live birth by a previous partner. The mean number of previous live births was 0.27 ± 0.5.

Gestational age was calculated based on basal body temperature charts. Ultrasonography was performed once a week from 4 to 8 weeks of gestation. Dilation and curettage was carried out when miscarriages were diagnosed, and the karyotypes of aborted conceptuses were determined using a standard G-banding technique.

The 82 fertile women with no history of recurrent miscarriage and complications of pregnancy were examined as controls. The fertile controls were recruited in Nagoya City University Hospital and Asamoto Women's Clinic. The mean age of women in the control group was 32.3 ± 6.2 years, and the average number of deliveries was 1.53 ± 0.6.

The study was approved by the Research Ethics Committee of Nagoya City University Graduate School of Medical Sciences. Each patient provided their written consent after full disclosure about the purpose and methods to be employed.

DNA analysis

Genomic DNA was extracted from peripheral blood samples with the Midi Blood DNA Extraction kit (Qiagen, Tokyo, Japan). Oligonucleotide primers were designed to amplify each coding sequence, as well as exon–intron boundaries of the human *SYCP3* gene, encompassing exons 7–9 (GenBank accession number NM_153694). The sense and antisense PCR and sequence primers for *SYCP3* were, respectively, 5′-GATGGCGTG TGCCTATAATCCAAG-3′ and 5′-CGTCTTTATTTAATTGACAGTGT TAG-3′. Additional direct sequence primers were 5′-GTCAT GTTGCTCAGGCTGGTC-3′, 5′-TCTGTGGATTGATAATTATCTACT G-3′, 5′-TCCAATGCTCTGAGAACC-3′ and 5′-TCACCACAGC AAGTTGTG-3′. The coding exons 7–9 and exon–intron boundaries of human *SYCP3* gene were amplified by PCR and sequenced using the Big Dye Terminator v3.1 Cycle Sequencing kit (ABI Prism, Applied Biosystems, Foster City, CA, USA) on a 3100 automated sequencer.

Results

Heterozygous 657T>C mutation in exon 8 of *SYCP3* was ascertained in one of 101 patients who had had six recurrent miscarriage and in one of the 82 fertile controls (Fig. 1). The IVS7-16_19 delACTT previously reported in one patient with recurrent miscarriage or 643delA previously reported in two patients with azoospermia was not found in any patients with recurrent miscarriage or in fertile controls. No other new mutation was found in patients with recurrent miscarriage or controls.

Thirty-two patients experienced miscarriage with a normal embryonic (fetal) chromosome karyotype, and 47 patients presented an abnormal embryonic (fetal) karyotype (Table I). Two patients had miscarriages with both normal and abnormal karyotype.

Patient No. 77 with the 657T>C mutation was 31 years old and experienced a total of six miscarriages and no live birth. Available fetal karyotypes were shown as 46, XX and 46, XY. The control with the 657T>C mutation had a history of one live birth and no miscarriage.

Nine patients (No. 39–47) had repeated miscarriage with an abnormal karyotype, and seven patients (No. 75–81) had repeated miscarriage with a normal karyotype. Only 2 out of 18 (11.1%) patients had experienced miscarriages with both abnormal and normal embryonic karyotypes.

Discussion

In the present study, we found a heterozygous 657T>C mutation in exon 8 of the *SYCP3* gene in one patient and one fertile control. We could not find the IVS7-16_19 delACTT reported in one patient with recurrent miscarriage or 643delA reported in two patients with azoospermia in any patients with recurrent miscarriage or in fertile controls (Miyamoto et al., 2003; Bolor et al., 2009). No other new mutation was found in patients with recurrent miscarriage or controls.

Bolor et al. (2009) reported that 7.7% (2 of 26) patients with unexplained recurrent miscarriage were found to carry independent heterozygous nucleotide alterations, IVS7-16_19delACTT and 657T>C in *SYCP3*, neither of which was present among a control group of 150 fertile women. They also reported that analysis of transcripts from minigenes harboring each of these two mutations revealed that both mutations affected normal splicing, possibly resulting in the

Table I Previous miscarriage, live birth and subsequent pregnancy outcome with karyotype analysis (n = 101 patients).

Pt.	Prior history			Age (year)	Subsequent pregnancy			Karyotype	Cumulative live birth
	No. of P.M.	No of L.V.	Karyotype of previous miscarriage		Outcome		Karyotype of miscarriage		
1	2	2		37	f		47,XX,+16	A	y
2	3	0	#3 47,XY,+16	34	s	s		A	y
3	4	1		39	f		47,XX,+22	A	y
4	2	1		37	f	s	47,XX,+21	A	y
5	2	0		38	f	s	48,XX,+8,+22	A	y
6	3	0		28	f	s	47,XY,+16	A	y
7	3	0	#3 69,XXY	34	s			A	y
8	4	1	#3 47,XY,−13,+i(13)(p10),+i(13)(q10)[11]/46,XY,−13,+i(13)(q10)[19]	33	no			A	y
9	4	1	#2 47,XY,+18 stillbirth 32w	32	s			A	y
10	2	0		31	f	s	47,XX,+22	A	y
11	3	0	#3 45,X	42	s			A	y
12	4	1	#4 48,XY,+10,+13[12]/47,XY,+13[8]	35	no			A	y
13	3	0	#3 47,XX,+12	40	s			A	y
14	4	0	#4 46,XY,5cenh+,add(8)(p23)[7]/46,XY,5cenh+[13]	32	s			A	y
15	4	1	#3 47,XY,+7	38	s			A	y
16	4	1	#4 47,XY,+3	34	no			A	y
17	3	1	#3 47,XY,+16	36	s			A	y
18	4	0	46,XX,del(6)(q27)[12]/46,XX,add(6)(q27)[3]/46,XX,add(6)(q27)[2]/	37	s		46,XX,der(6)t(1;6)(q11;q27)[2]/46,XX,der(6)t(6;9)(q27;q12)[1]	A	y
19	2	0		33	f	s	48,XX,+15,+20	A	y
20	3	0	#3 45,XY, −21	30	f	s	ND*	A	y
21	3	1	#3 45,X	32	no			A	y
22	2	0	#2 47,XX,+22	32	f	s		A	y
23	3	1		40	f	s	48,XX,+14,+15	A	y
24	3	0	#3 47,XY,+16	31	s			A	y

Continued

Table I *Continued*

Pt.	Prior history			Age (year)	Subsequent pregnancy			Karyotype	Cumulative live birth
	No. of P.M.	No of L.V.	Karyotype of previous miscarriage		Outcome		Karyotype of miscarriage		
25	4	0	#3 47,+22	39	s			A	y
26	2	0		37	f		47,XY,?	A	n
27	3	0		34	f		47,XY,+16	A	n
28	2	0		39	f		47,XX,+16	A	n
29	2	0		32	f		47,XY,+16	A	n
30	5	0	#5 46,X,+16	27	f		Bio Misc	A	n
31	3	0		28	f		47,XX,+13	A	n
32	5	0		46	f		47,XX,+22	A	n
33	3	0	#3 47,XX,add(2)(q37),+20	42	no			a	n
34	4	0	#1 stillbirth 16w; #4 47,XY,+15	39	no			a	n
35	3	0		41	f		47,XX,+16	a	n
36	4	0		43	f		48,XY,+16,+21	a	n
37	4	0		38	f		46,X,+3	a	n
38	6	0	#1 stillbirth 33w; #4 45,X	37	no			a	n
39	7	0	#5 47,XX,+16; #7 45,X	30	s			aa	y
40	6	0	#6 47,XY,+16	32	f	s	47,XX,+13	aa	y
41	2	1	47,XY,+21***	30	f		47,XX,+5	aa	y
42	3	0	#3 47,XX,+16	29	f	s	47,XX,+3	aa	y
43	6	1	#6 47,XX,+16	41	f		47,XX,+12	aa	y
44	2	0	#2 46,XY,add(8)(p23)	33	f		47,XY,+16	aa	n
45	4	0	#2 45,X; #4 47,XX,+idic(8)(q?21.2)	35	no			aa	n
46	2	0		30	f	f	47,XX,+15;45,X	aa	n
47	2	0	#2 47,XX,+15	35	f		45,X	aa	n
48	14	2	#12 47,XX,+16 #14 46,XY, 2 children with previous husband	45	no			an	y
49	4	1	#3 47,XY,+16;#4 46,XX	30	f		46,XY	ann	y
50	4	0	#4 46,XY	35	s	s		n	y
51	4	0	#1 Stillbirth 28w; #4 46,XX	28	s		On-going preg.EDC06/27/11	n	y
52	4	0	#3 Stillbirth 18w	35	f	s	46,XY stillbirth 33w	n	y
53	3	0	#3 46,XY	33	s			n	y
54	5	1	#5 46,XY	36	s			n	y
55	4	1	#3 46,XY	36	no			n	y

56	3	0	#3 46,XX	30	s				n	y
57	3	0	#3 46,XX	32	s				n	y
58	2	0		34	f	s		46,XX	n	y
59	3	1	#3 46,XX	35	no				n	y
60	3	1	#3 46,XX	33	s				n	y
61	4	0	#4 stillbirth 15w	37	f	s		46,XX stillbirth 13w	n	y
62	3	0	#3 46,XX	33	s				n	y
63	3	1	#3 46,XY	37	s				n	y
64	3	0		26	f			46,XX	n	n
65	3	0		34	f			Normal Karyotype	n	n
66	5	0	46,XY	40	no				n	n
67	2	0		32	f			46,XX	n	n
68	3	0	#3 46,XY	35	f			NT**	n	n
69	2	0		39	f			46,XX	n	n
70	3	0	#3 46,XX	28	no				n	n
71	2	0		36	f			46,XX	n	n
72	2	0		30	f			46,XY	n	n
73	3	0	#3 46,XX	34	no				n	n
74	2	0		31	f			46,XY	n	n
75	3	0	#2 46,XX; #3 46,XY	31	s				nn	y
76	2	0	#2 46,XY	22	f	s		46,XY; On-going preg.EDC 05/27/11	nn	y
77	5	0	#5 46,XY	31	f			46,XY	nn	n
78	5	0	#3 46,XX; #4 46,XY; #5 46,XY	36	f	f	s	46,XX,t(11;19)(q21;q13.1) [4]/46,XX[26], Bio Misc	nnnn	y
79	6	0	#3#,4#,6 46,XX,inv(9); #5 46,XY,inv(9)	31	s			On-going preg.EDC 02/23/11	nnnn	y
80	9	0	#5 46,XX;#6 46,XX;#8 46,XY	38	f			46,XX	nnnn	n
81	13	0	#4 46,XY; 46,XX; 46,XX; 46,XX	33	f	f	f	46,XX; 46,XX; 46,XX	Nnnnnnn	n
82	3	0		31	s					y
83	3	0		39	s					y
84	3	0		26	s					y
85	3	0		38	s					y
86	23	0		33	s					y
87	3	1		35	f			Bio Misc		y
88	3	0		28	s					y
89	3	0	#2 stillbirth 15w	30	s					y
90	3	1		35	no					y

Continued

Table I *Continued*

Pt.	Prior history			Age (year)	Subsequent pregnancy		Karyotype	Cumulative live birth
	No. of P.M.	No of L.V.	Karyotype of previous miscarriage		Outcome	Karyotype of miscarriage		
91	3	2	2 children with previous husband	34	s			y
92	3	1		38	s	On-going preg.EDC03/24/11		y
93	3	0		36	s			y
94	5	0		34	f	ND*		n
95	2	0		28	f	Bio Misc		n
96	4	0		41	no			n
97	4	0		42	no			n
98	3	0		33	no			n
99	4	0		31	no			n
100	3	0	#1 stillbirth 18w; #3 stillbirth 23w	32	no			n
101	4	0		37	f	Bio Misc		n
	3.782178	0.267327		34.347				
	2.681805	0.507762		4.4033				

*ND, not detected; **NT, not tested; ***Live birth, He is 8 years old; Pt., patient; P.M., previous miscarriage; L.V., Live Birth; Bio Misc, biochemical miscarriage, decreasing hCGs < 1500 mIU/ml; age, age at examination karyotype; a, aneuploidy; n, normal karyotype (euploidy) from Pt. 1–81, karyotype were knowed in prior history or subsequent pregnancy; 'Outcome' reflect the conclusion of subsequent pregnancy; 's' means success in live birth delivery; 'f' means failure, miscarriage.